Tuning the Surface State Dimensionality of Cu Nanostripes

J. Lobo,[1] E. G. Michel,[1] A. R. Bachmann,[2] S. Speller,[2] J. Kuntze,[3] and J. E. Ortega[4,5]

[1]*Departamento de Física de la Materia Condensada and Instituto Universitario de Ciencia de Materiales "Nicolás Cabrera," Universidad Autónoma de Madrid, 28049 Madrid, Spain*

[2]*Institute for Molecules and Materials, Radboud University Nijmegen, Toernooiveld 1, 6525 ed Nijmegen, The Netherlands*

[3]*Institut für Experimentelle und Angewandte Physik, Olshausenstrasse 40, D-24098 Kiel, Germany*

[4]*Universidad del País Vasco, Departamento Física Aplicada I, Plaza Oñate 2, E-20018 San Sebastián, Spain*

[5]*Centro Mixto CSIC/UPV and DIPC, Manuel Lardizabal 4, 20018-San Sebastian, Spain*

(Received 25 February 2004; published 24 September 2004)

Stepped Cu nanostripes with varying terrace widths are self-assembled during Ag-induced periodic faceting of vicinal Cu(111). By changing Ag coverage the average terrace size within individual Cu stripes is readily tuned, making it possible to select the one-dimensional or two-dimensional character of surface states. Furthermore, the average terrace size can be smoothly switched from 10 to 30 Å, thereby tracking the transition from step-lattice, quasi-two-dimensional umklapp bands to terrace-confined one-dimensional quantum well states.

DOI: 10.1103/PhysRevLett.93.137602 PACS numbers: 79.60.Bm, 68.35.Bs, 73.21.–b, 78.66.Bz

The ability of tailoring electronic states in nanostructures is of technological and fundamental importance. Quantum size effects trigger a variety of exotic phenomena, such as oscillatory magnetic coupling [1], structural transitions [2], or even crystal growth [3]. It is also a major challenge to prove exciting predictions for one-dimensional (1D) systems like spin-charge separation in Luttinger liquids [4]. Noble metal surfaces featuring a surface state are especially appealing substrates to engineer 1D and 2D nanostructures. The strong scattering of surface state electrons at adatoms, defects, and steps gives rise to interference patterns that can be readily studied, e.g., by scanning tunneling microscopy (STM) [5–7]. In particular, vicinal surfaces with 1D arrays of monatomic steps are attractive to investigate electronic states of self-assembled 1D superlattices [8]. The terrace width d is the lattice constant, which is tuned macroscopically by changing the miscut angle, i.e., the deviation of the surface plane from the high symmetry direction of the terraces. Furthermore, in noble metal surfaces it is possible to tailor surface states by simply changing d, switching from 2D step-superlattice bands to 1D confinement and quantum well (QW) states [9–14]. This has recently raised exciting issues in low-dimensional systems, like the ability of mapping real space wave functions in 1D quantum wells [7,15], and the possible structural stability of a given terrace width due to Fermi level gap opening in vicinal Cu(111) [v-Cu(111)] [13].

In this Letter we present a very handy system to further investigate the changing nature of electronic states in step arrays with different lattice constants, namely, self-assembled stepped Cu nanostripes. These are produced by periodic faceting of v-Cu(111) during Ag adsorption and annealing [16]. The side view of the system is shown in Fig. 1. The periodic hill-and-valley structure is made of close-packed Ag-covered facets and stepped Cu stripes. Interestingly, by simply varying the Ag coverage one can smoothly switch the local miscut of the Cu nanostripe with respect to the (111) direction, i.e., the average terrace width. We have analyzed the electronic states of such nanostripes using angle-resolved photoemission. Despite their finite size, we find a close analogy with bulk v-Cu(111) crystals of the same miscut. This has allowed us to monitor in detail the transition from quasi-two-dimensional (2D) umklapp bands for 17 Å step-lattice distance [Fig. 2(b)] to 1D quantum well states confined within 30 Å wide Cu terraces [Fig. 2(c)]. This transition is characterized by a diminishing spectral intensity inside the step-superlattice band gap, also observed in bulk crystals [9–14], supporting the claim of a progressive change in the spectral weight of 1D and 2D surface state Fourier components [8].

The substrate is Cu(111) with $\theta_0 = 11.8°$ miscut towards the $[\bar{1}\,\bar{1}\,2]$ direction. The clean surface displays

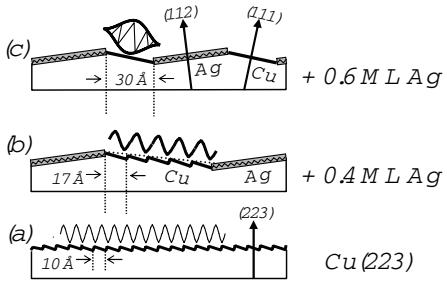

FIG. 1. Schematic side view of Ag-faceted periodic nanostructures. By increasing the Ag coverage, one can tune the average terrace size in the Cu nanostripes, such that it is possible to switch from (a) the extended step array of the Ag-free substrate with 10 Å terraces to (b) quasi-2D superlattice states in 17 Å terraces, and to (c) 1D quantum well states in 30 Å terraces.

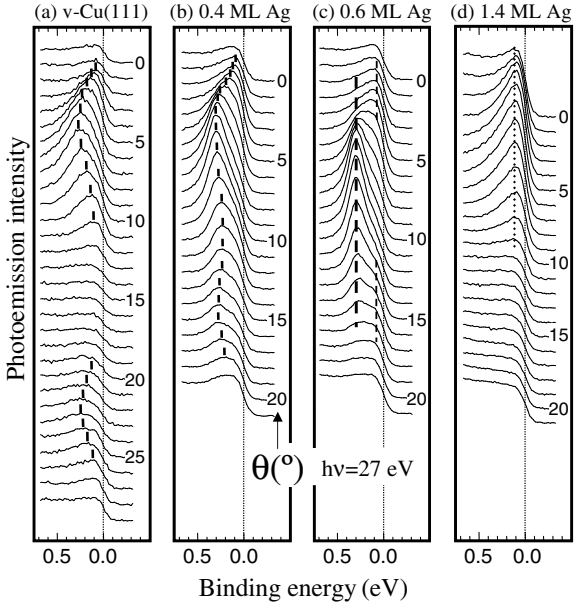

FIG. 2. Angle-resolved, valence band photoemission spectra for Ag/Cu lateral nanostructures with increasing Ag coverage from (a) to (d). The surface state dispersion is measured along the $[\bar{1}10]$ direction (perpendicular to the steps of the substrate). In (a) and (b) the ticks indicate the peak position. Analogous to the findings for bulk vicinals, the Cu surface state evolves from a 2D step-superlattice in (a) through a quasi-2D state with a large gap in (b) to a 1D quantum well state in (c). (d) Beyond 1 ML, only a Ag derived state is seen.

regular arrays of linear, monatomic steps that separate (111)-oriented, $d = 10.0 \pm 1.5$ Å wide terraces, as determined by STM [11,16]. The experiments have been performed at the SU8 undulator beam line at LURE (Orsay, France), with a total energy resolution of 80 meV, angular resolution of $\pm 0.5°$, and 70° incident light. The Ag/Cu striped structure is produced by deposition of Ag at 300 K and annealing to 420 K. The detailed growth morphology is studied in Ref. [16]. As shown in Fig. 1, up to $\sim$0.6 monolayers (ML) we have regular arrays of Ag-covered (112)-oriented facets and Cu stepped stripes. The characteristic low-energy electron diffraction (LEED) pattern with sharp split spots of Cu stripes allows one to determine the Ag coverage (± 0.05 ML) and the average terrace width d^* within Cu nanostripes [16]. Up to 0.6 ML Ag-covered (112) facets grow laterally leading to step removal from Cu stripes, such that the average terrace width within the stripe d^* increases as a function of coverage. Beyond 0.6 ML, Ag-covered (335) stripes start to nucleate inside (112) facets. Above 1 ML, large (335) patches and random (223) steps completely cover the surface.

Figure 2 shows the angle-resolved photoemission spectra from 2(a) clean v-Cu(111) and after deposition and annealing of 2(b) 0.4 ML, 2(c) 0.6 ML, and 2(d) 1.4 ML of Ag. The emission angles refer to the average surface normal. We observe two distinct Ag-like and Cu-like features that are readily assigned from the coverage dependence. The Ag peak, which is cut off by the Fermi level, is only visible beyond 0.6 ML, as in Fig. 2(d). The interest is focused on Figs. 2(a)–2(c), where the features correspond to surface states of Cu nanostripes. We observe a strong qualitative similarity with surface states of v-Cu(111) and v-Au(111) with the same miscut [9–14]. In particular, by increasing d^* in Cu stripes we also observe the switch from a dispersing 2D surface state in the infinite surface in Fig. 2(a) to the terrace-confined 1D QW in Fig. 2(c), passing through the intermediate case of a 2D step-superlattice state with an apparent large gap opening at the superlattice zone edge in Fig. 2(b).

The quantitative analysis confirms the analogy with the bulk crystals. The clean surface spectra in Fig. 2(a) display the step-superlattice umklapp [11]. The band minima at $E_b = -0.26$ eV are split by $\delta\theta = 15.5°$, which corresponds to $\Delta k_x = [(2m_e/\hbar^2)E]^{1/2} \sin\delta\theta = 0.65$ Å^{-1}, in agreement with the step-lattice vector $2\pi/d = 0.63$ Å^{-1} (E refers to the photoelectron kinetic energy). For 0.4 ML we still observe 2D-like surface peak dispersion, with two shallow minima at $E_b = -0.32$ eV split by $\delta k_x = 0.39$ Å^{-1}. Both the reduced umklapp and the upwards energy shift are explained by a wider $d^* = 17$ Å terrace ($2\pi/d^* = 0.37$ Å^{-1}), and are consistent with data from the corresponding infinite Cu(443) surface [13]. Despite the finite size ($w = 60$ Å) of the Cu nanostripe, which indeed introduces an additional spectral broadening along k_x, $\Delta k_x = \pi/w = 0.05$ Å^{-1} [17], the spectra in Fig. 2(b) display the same overall features observed in Cu(443). This supports the idea of a short electron coherence length in step arrays [13], which makes infinite crystals and nanostripes effectively equivalent.

For 0.6 ML the Cu peak evolves into a strong nondispersive, QW feature at $E_b = -0.30$ eV, and two less intense peaks close to E_F at low and high emission angles. The similarity with the Au(887) spectra in Ref. [9] allows us to assign features to the $N = 1$ and 2 quantum well states of terraces. The energy shift of the $N = 1$ peak with respect to the Cu(111) surface state indicates an average terrace width $d^* = \sqrt{(\hbar^2\pi^2)/(2m^*(E_b - E_0))} = 30$ Å ($m^* = 0.45m_e$, $E_0 = -0.39$ eV [18]). This value is in turn consistent with the $N = 2$ level located 20 meV below E_F, and hence cut off by the E_F edge, as indicated in Fig. 2(c). Note that d^* in this case appears to be an effective terrace width, since at 0.6 ML the STM images show 40 Å wide Cu stripes with random steps pinned by adjacent Ag facets [16]. Data in Fig. 2(c) can be compared with the Cu(665) case (25 Å terraces), where 1D QWs have also been claimed [14]. The nanostripe displays sharper QW features than Cu(665) and no residual dispersion. This is not due to a reduced terrace width broadening (TWD), which is probably larger in the present

case, but it is rather explained by a much better defined 1D behavior with 30 Å terraces, as we discuss later.

The surface state wave function properties of Cu nanostripes are further tested in the photon-energy analysis shown in Fig. 3. For different coverages we show in a gray scale the normalized photoemission intensity as a function of electron binding energy and emission angle. For a better observation, the Fermi edge has been deconvoluted and removed from the spectra. As in LEED [19], the intensity peaks for in-phase interference and the band (spot) splitting is observed near out-of-phase conditions [8]. We mark the center of the different spots with white lines. The respective (k_x, k_z) values are plotted in Fig. 3(d) with different symbols [20]. This plot allows one to probe the Fourier components of the surface state and their broadening direction in the plane of Fig. 1, which in turn determines the so-called modulation plane of the wave function [10]. First and second Brillouin zone data are fitted separately with straight lines in each case. For the clean surface both split rods ($2\pi/d = 0.63$ Å^{-1}) line up perpendicular to the surface plane. For 0.4 ML the two split rods ($2\pi/d^* = 0.37$ Å^{-1}) are tilted by $\alpha = 5°$ with respect to the average surface normal, whereas for 0.6 ML the broadening direction further rotates to $\beta = 13°$. The former corresponds to the local surface normal of the Cu stripe, and the latter is very close to the Cu(111) terrace orientation (12° with respect to the average surface). Thus, as schematized in Fig. 1, Cu nanostripe states are, respectively, modulated with respect to the stripe plane in the quasi-2D superlattice states of Fig. 1(b), and with respect to the (111) terrace plane for 1D quantum well states of Fig. 1(c).

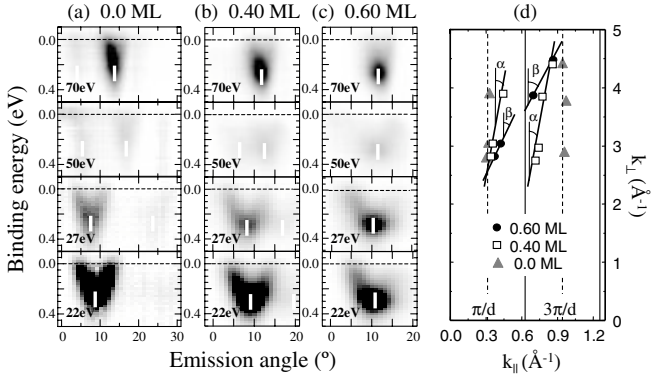

FIG. 3. Surface states as a function of photon energy for (a) clean v-Cu(111), (b) 0.40 ML Ag, and (c) 0.60 ML Ag, shown in a gray scale. White vertical lines mark the center (θ_c) of the surface state band. (d) Corresponding $k_x - k_z$ plot. The points correspond to the photoemission wave vector components at θ_c. Data points line up at different angles (α, β) that correspond to the average surface [clean v-Cu(111), local stripe (0.4 ML)] or terrace (0.6 ML) orientation with respect to the substrate plane.

In Fig. 4 we closely look at the transition from 2D to 1D surface states in nanostripes. In order to enhance peak features we represent the second derivative of the photoemission spectra in a gray scale [8]. The Fermi edge was previously removed to prevent artificial features at that energy. The data have been taken at the same $h\nu = 27$ eV photon energy, such that the same Fourier components are probed. The system goes from the ~60 Å nanostripe with 3–4, 17 Å terraces in 4(a) to the single ~30 Å terrace in 4(c), passing through an intermediate ~50 Å wide stripe with two ~25 Å terraces at 0.5 ML in 4(b). Thus, the latter is comparable to Cu(665) [14]. For 17 and 25 Å terraces there is dispersion and umklapp with the expected (within error bars) lattice vectors $2\pi/d^* = 0.36$ and 0.23 Å^{-1}, respectively. There is also a residual dispersing intensity that connects lower bands and Fermi energy features, filling the superlattice band-gap region, as observed in Cu(443) and Cu(665). For the 30 Å terrace, which is the only clear-cut 1D state case in Fig. 4, no such residual intensity is found within the QW gap. One cannot explain the residual dispersing band by TWD broadening, since we find a similar TWD for 0.4 and 0.5 ML, and an even broader distribution for 0.6 ML. The overall behavior in Fig. 4 is straightforwardly explained by a very smooth, progressive transition from 2D resonances to 1D states. This is characterized by a complex, step-distance-

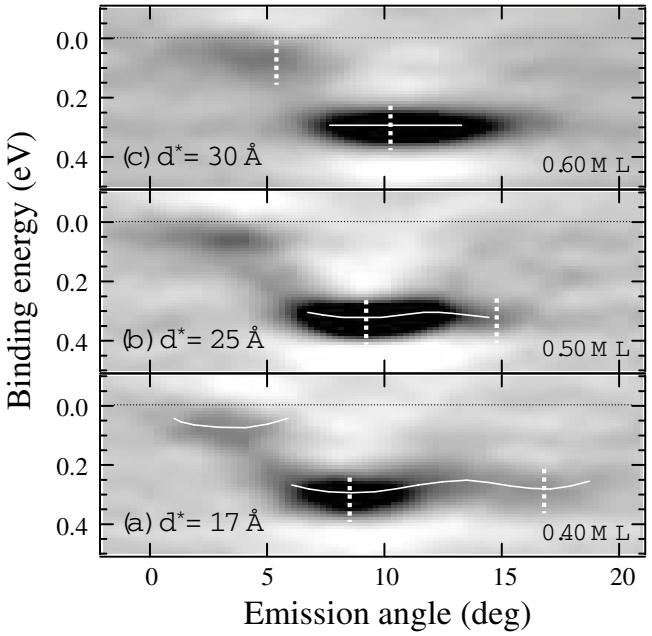

FIG. 4. Transition from 2D to 1D states in Cu nanostripes. The second derivative of the photoemission intensity is shown to enhance dispersive features. White lines and ticks, respectively, mark band dispersion and minima in (a) and (b), whereas in (c) they indicate peak position and intensity maxima for the $N = 1$ and 2 QWs, respectively. Dispersion and umklapp are observed for (a) 17 Å and (b) 25 Å terraces. A clear gap is present only in (c) for 30 Å terraces.

dependent Fourier spectrum for intermediate miscut angles, with partial mixing with bulk states, until the bulk *s, p* gap fully develops [8,21]. The progressively vanishing intensity inside the gap in Figs. 4(a) and 4(b) appears to be the signature of such mixing. The bulk-surface state overlap nominally occurs at miscut angles larger than $\theta_c = \tan^{-1}(k_{\text{neck}}/2k_L)$, where k_{neck} and k_L stand for the constant energy surface neck radius and the bulk ΓL distance, $k_L = 1.51$ Å^{-1}, respectively [8]. At $E = (E_F - 0.3)$, $k_{\text{neck}} = 0.21$ Å^{-1} [22]; thus $\theta_c = 4°$, and hence the critical terrace width is 30 Å. For nanostripes the bulk projection picture appears less appropriate, and one should rather think in terms of the minimum step-lattice vector $2\pi/d^*$ that couples surface and bulk states [10,23]. This also gives the same critical miscut [10]. A decreasing coupling to bulk states involves a shorter penetration depth of the surface wave function inside the crystal [8]. The penetration depth can be estimated from the width of the cross section resonance around the L point [24]. To this aim, we have performed photon-energy dependent experiments that display a broad, structured peak, probably due to a complex final-state band structure around L [24], which renders a line shape analysis impossible. Looking at Fig. 4, the gap opening at E_F for 17 Å terraces as reported in Ref. [13] appears questionable here. The angular and photon-energy dependence of the spectral intensity must be taken into account, e.g., for the umklapps in Fig. 4(a). Those located on the right side are barely seen, but the left umklapp is clear. Its relative intensity with respect to the main band is comparable to the relative intensity of the $N = 2$ QW peak [which is observed at the same emission angle in Fig. 4(c)] with respect to $N = 1$. Since the $N = 2$ state is located below E_F, we could say that the umklapp band in Fig. 4(a) should not be above E_F. Thus, the band gap in Fig. 4(a) appears to open below the Fermi energy.

In summary, Ag-induced faceting of vicinal Cu(111) allows the engineering of vicinal Cu nanostripes with tunable step spacing. These nanostripes display surface states analogous to the respective infinite vicinal surfaces with the same miscut angle, supporting the idea of a reduced electron coherence length in stepped crystals. We have focused on the transition from two-dimensional surface umklapp bands to one-dimensional lateral quantum well states, which we find to be smooth, as expected from a reduced mixing of surface and bulk states as terraces become larger. Pure 1D surface states are found only with 30 Å terraces. The data do not reflect a clear Fermi level band gap for 17 Å terraces. Nonetheless, the system appears ideal for future STM or spot-profile LEED investigations on this issue, i.e., on the structural stability of step arrays as a function of electronic states.

J. L., E. G. M., and J. E. O. are funded by the Spanish Ministerio de Ciencia y Tecnología (BFM2001-0244, MAT2002-03427, MAT-2002-11975-E, HA2002-0107), the Universidad del País Vasco (1/UPV/EHU/00057.240-EA-13668/2001). A. R. B. and S. S. are supported by the Stichting voor Fundamenteel Onderzoek der Materie (FOM) and the Deutsche Forschungsgemeinschaft (DFG). E. G. M., J. K., and J. E. O. acknowledge support from the European Science Foundation. We thank F. Ostendorf, L. Roca, and the staff of SU8 beam line for help during the experiments.

[1] F. J. Himpsel *et al.*, Adv. Phys. **47**, 511 (1998).
[2] Z. Zhang *et al.*, Phys. Rev. Lett. **80**, 5381 (1998); P. Czoschke *et al.*, Phys. Rev. Lett. **91**, 226801 (2004).
[3] N. Memmel and E. Bertel, Phys. Rev. Lett. **75**, 485 (1995); M. Giesen *et al.*, Phys. Rev. Lett. **82**, 3101 (1999).
[4] J. Voit, Rep. Prog. Phys. **58**, 977 (1995).
[5] M. F. Crommie *et al.*, Nature (London) **363**, 524 (1993).
[6] Ph. Avouris and I.-W. Lyo, Science **264**, 942 (1994).
[7] L. Bürgi *et al.*, Phys. Rev. Lett. **81**, 5370 (1998).
[8] A. Mugarza and J. E. Ortega, J. Phys. Condens. Matter **15**, S3281 (2003).
[9] A. Mugarza *et al.*, Phys. Rev. Lett. **87**, 107601 (2001); J. E. Ortega *et al.*, Phys. Rev. B **65**, 165413 (2002).
[10] J. E. Ortega *et al.*, Phys. Rev. Lett. **84**, 6110 (2000).
[11] J. Lobo *et al.*, J. Vac. Sci. Technol. A **21**, 1194 (2003).
[12] F. Baumberger *et al.*, Phys. Rev. B **64**, 195411 (2001).
[13] F. Baumberger *et al.*, Phys. Rev. Lett. **92**, 016803 (2004).
[14] F. Baumberger *et al.*, Phys. Rev. Lett. (to be published).
[15] A. Mugarza *et al.*, Phys. Rev. B **67**, 081404 (2003).
[16] A. R. Bachmann *et al.*, Surf. Sci. **526**, L143 (2003).
[17] J. E. Ortega *et al.* (to be published).
[18] R. Paniago *et al.*, Surf. Sci. **336**, 113 (1995).
[19] M. Henzler, Appl. Phys. A **9**, 11 (1976).
[20] k_z is determined in the free-electron-like final-state approach from the measured k_x and kinetic energy E via $k_z = [(2m_e/\hbar^2)(E + V_0) - k_x^2]^{1/2}$, where $V_0 = -13.5$ eV is the crystal inner potential.
[21] R. Eder and H. Winter, Phys. Rev. B **70**, 085413 (2004).
[22] F. Reinert *et al.*, Phys. Rev. B **63**, 115415 (2001).
[23] G. Hörmandinger and J. B. Pendry, Phys. Rev. B **50**, 18 607 (1994).
[24] S. D. Kevan and R. H. Gaylord, Phys. Rev. Lett. **57**, 2975 (1986).